Low-dose computed tomography as diagnostic tool in calcium pyrophosphate deposition disease arthropathy: focus on ligamentous calcifications of the wrist

K. Ziegeler[1], T. Diekhoff[1], S. Hermann[2], B. Hamm[1], K.G.A. Hermann[1]

[1]Department of Radiology, [2]Department of Rheumatology and Clinical Immunology, Charité - Universitätsmedizin Berlin, Germany.

Abstract

Objective

To identify specific morphologic features of calcium pyrophosphate deposition disease (pseudogout, CPPD) manifestations of the wrist as detected using low-dose CT-scans.

Methods

In this retrospective study 46 patients with arthritis of the wrist were included. All patients underwent a low dose CT scan of both wrists on a 320-row detector in volume scan mode. Individual radiation exposure was recorded for all patients. Two blinded raters independently evaluated osteoarthritis, cysts, erosions, calcifications (cartilage and ligaments separately) and carpal misalignment in 33 specified locations. An expert rheumatologist classified the patients as CPPD positive or negative. Fisher's exact test was applied to identify differences between both groups. Receiver operating characteristics (ROC) analyses with calculations of area under the curve (AUC) were carried out for both in the literature established and newly identified imaging findings for each rater individually.

Results

Twenty-seven patients were classified as CPPD, 19 patients as other diagnoses. Ligamentous calcifications were significantly more prevalent in the CPPD group ($p<0.05$). All non-ligamentous findings revealed no difference in frequency. AUC analysis for established findings (0.675; 0.619 - rater 1; 2) vs. ligamentous calcifications (0.786 both raters) showed a markedly higher diagnostic accuracy for the latter. Effective radiation exposure was determined to be 0.019–0.095 mSv per patient.

Conclusion

Calcifications of carpal ligaments are highly specific morphologic features of CPPD arthropathy. Low-dose CT is a useful tool to detect these calcifications at a radiation exposure similar to a standard radiograph.

Key words

calcium pyrophosphate deposition disease, computed tomography, arthropathy

Katharina Ziegeler, MD
Torsten Diekhoff, MD
Sandra Hermann, MD
Bernd Hamm, MD, PhD
Kay Geert A. Hermann, MD, PhD

Please address correspondence to:
Dr Kay Geert A. Hermann,
Charité - Universitätsmedizin Berlin,
Department of Radiology (CCM),
Charitéplatz 1,
10117 Berlin, Germany.
E-mail: kghermann@gmail.com

Received on September 19, 2018; accepted in revised form on December 3, 2018.

Competing interests: K.G.A. Hermann has received honoraria from Abbvie, Merck, Novartis, Pfizer and UCB. The other co-authors have declared no competing interests.

Introduction

The deposition of calcium pyrophosphate dihydrate crystals (CPPD) is the basis of a form of arthritis with a wide spectrum of clinical manifestations (1). In the past a number of different terms, including the still popular 'pseudogout', has been used to describe subsets of this illness – a recently formed taskforce of the European League Against Rheumatism (EULAR) has suggested the term CPPD for all instances of CPP-deposition, however, which will therefore be adopted in this study (2). CPPD has been estimated to be the third most common form of inflammatory arthritis with a prevalence of up to 0.42% (3) and is particularly prevalent in the elderly (4).

Manifestations especially at the hand and wrist can be difficult to diagnose, due to a clinical appearance similar to other arthritides (5). The standard of reference for the diagnosis of CPPD is the identification of the characteristic weakly birefringent crystals in the synovial fluid of an affected joint (2). This standard however, can be very challenging to meet in a regular outpatient setting, due to lack of training and punctio sicca at times (6). Additionally the reliability of routine laboratory analyses of synovial fluid in regard to pyrophosphate crystals has been called into question (7).

Thus the diagnosis of CPPD often relies strongly on imaging findings, especially on radiography (8). Common radiographic findings in CPPD wrist arthropathy include osteoarthritis (OA) especially of the scapho-radial and scapho-trapezio-trapezoideal (STT) joint (9, 10) and drooping osteophytes (also referred to as 'hook-shaped osteophytes') of the metacarpophalangeal (MCP) joints (11). Typical of this condition are calcifications of hyaline and fibrocartilage, which inspired the alternative term 'chondrocalcinosis' for the deposition. In CPPD manifestations of the wrist and hand, these calcifications are typically found at the triangular fibrocartilage and the lunotriquetral ligaments and cartilage (12). Another common finding are cystic lesions – these are most commonly reported in the scaphoid and lunate (13) and are typically very large in appearance. Additionally, scapho-lunate dissociation (14) and subluxation of the scaphoid (15) have been described in patients with CPPD. There are, however, certain limitations to the diagnostic accuracy of plain radiography. Calcifications of soft tissues other than those mentioned above for example, are difficult to detect due to superimposition.

To date, larger investigations into the use of computed tomography (CT) in the detection of CPPD have been limited to locations other than the wrist – namely the knee and the spine (16). For manifestations at the atlantoaxial joint, the crowned dens syndrome, CT is vital for securing a diagnosis (17). CPPD CT manifestations of the wrist have thus far only been investigated in case studies (18).

The aim of this study was to systematically investigate the pattern of imaging findings in CPPD wrist arthropathy as detected using CT, in comparison to those of clinically related arthritides, thus yielding specific imaging characteristics for the diagnosis of CPPD.

Materials and methods

Patients

Included in this retrospective analysis were all patients with wrist arthralgia or swelling suspected for crystal arthropathy and without history of trauma of the affected region who underwent a volume CT of the wrist between January 2011 and July 2014 at our institute. An expert rheumatologist (8 years of experience in rheumatology) assigned patients to the CPPD or control group based on anonymised clinical data, including laboratory findings and descriptions of radiographs from a senior radiologist (16 years of experience is musculoskeletal imaging), without access to CT images and reports. The basis for the assignment to the CPPD group were the McCarty Criteria (19). In cases of secondary CPPD (*e.g.* haemochromatosis, rheumatoid arthritis), patients were classified as controls. Thus, the current standard of care was simulated, while limiting any bias of the expert rheumatologists due to a possible recognition of their own patients. Excluded from the analysis were patients with an incomplete capture of the carpus in the

volume CT, and or missing or incomplete clinical data (n=6).

The ethics review board of Charité Medical School, Berlin, Germany, waived approval of this study due to its retrospective nature. All patients gave written informed consent to the scientific use of imaging and clinical data prior to CT scanning. The study was conducted in line with the principles laid out in the Declaration of Helsinki and its latest update as consented in Fortaleza, Brasil, in 2013.

Imaging technique

All patients underwent a low-dose dual-energy CT scan of both wrists using a 320-row CT scanner (Aquilion ONE and Aquilion ONE Vision, Canon Medical Systems, Japan) (20, 21). The scan was performed using 80 kVp, and 90 to 170 mA, and 135 kVp and 15 to 30 mA in Volume mode with a Z-axis coverage of 16 cm without table movement and fastest rotation time. For all evaluations reported, volume acquisitions at 80 kVp were used. Images were evaluated completely anonymised in 0.5 mm coronal, axial and sagittal multiplanar reconstructions in a sharp bone kernel. The effective radiation exposure was established using the dose-length products and a conversion coefficient (κ) of 0.0008 mSv / mGycm (22, 23).

Scoring system

In order to establish a structured scoring system a literature research was undertaken to identify all previously described imaging characteristics of CPPD wrist arthropathy. The search terms applied were "*(CPPD OR pseudogout OR chondrocalcinosis OR calcium-pyrophosphate) AND (hand OR wrist OR carpal*) AND (imag* OR radiograph* OR x-ray)*" without restrictions on publication date but only including articles on humans. The search found 225 matches (November 2014) of which 19 articles were classed as relevant based on their title (11-13, 15, 24-39). The imaging characteristics extracted from these articles were examined for relevance by an expert panel (KGH, TD) – as a characteristic with low relevance, pyrophosphate tophi (39) were excluded. Based on this literature a scoring system was established comprising osteoarthritis, drooping osteophytes, cartilage and ligamentous calcification, cysts, scaphoid subluxation and scapho-lunate dissociation. Additionally, erosions were included in the scoring system. These imaging characteristics were evaluated in 33 predefined locations of the wrist (Fig. 1) by two blinded raters separately (rater 1: specialised radiologist with 6 years image interpretation experience; rater 2: specially trained research student). Imaging characteristics were evaluated based on a grading system (Table I).

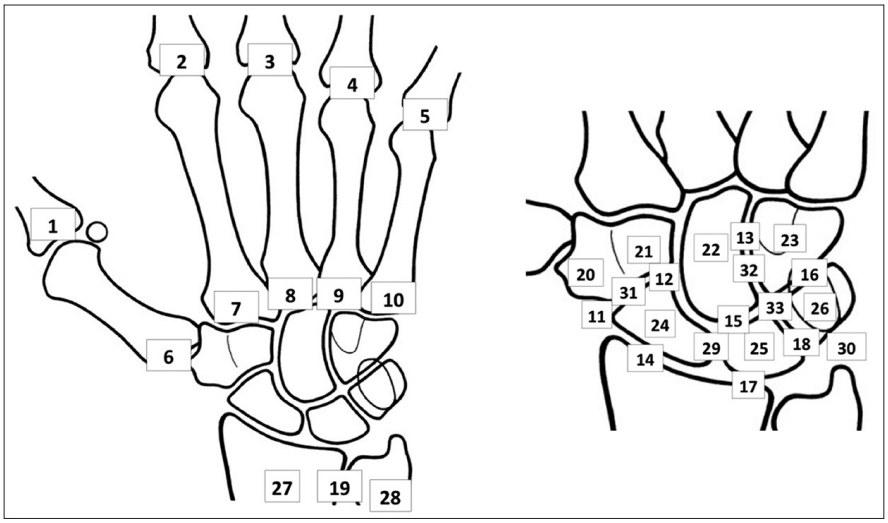

Fig. 1. Evaluated locations. Metacarpophalangeal joint (MCP)-I [1], MCP-II [2], MCP-III [3], MCP-IV [4], MCP-V [5], carpometacarpal joint (CMC)-I [6], CMC-II [7], CMC-III [8], CMC-IV [9], CMC-V [10], scaphotrapezio joint [11], scapho-trapezoideal joint [12], hamato-capital joint [13], scapho-radial joint [14], luno-capital joint [15], hamato-triquetral joint [16], luno-radial joint [17], luno-triquetral joint [18], distal radio-ulnar joint [19], trapezium [20], trapezoid [21], capitate [22], hamate [23], scaphoid [24], lunate [25], triquetrum/pisiforme [26], radius [27], ulna [28], scapho-lunate joint [29], triangular fibrocartilage [30], scapho-trapezio-trapezoideal joint [31], hamato capital joint [32], hamato-triquetro-luno-capital joint [33].

OA was evaluated based on the original classification by Kellgren and Lawrence (40). Scapho-lunate dissociation was defined as an increase in distance to at least 3 mm (15). For the detection of scaphoid subluxation the scapho-radial angle was measured in sagittal reconstructions - an increase to >70° was defined as a subluxation (15).

Additionally, each CT rater assigned the diagnosis '*CPPD*' or '*other arthritis*' to every patient based solely on the imaging findings. Prior to image evaluation a consensus reading with an expert radiologist was performed on two test cases. Based on the consensus scoring, a pictorial atlas was compiled for reference. To ensure a high degree of inter-rater reliability, both raters also independently performed two scorings on test patients prior to image evaluation.

Statistical analysis

The scoring sheets were digitalised using IBM SPSS v. 22 (IBM, Corporation, New York, USA). T-test for unpaired samples was applied to test for differences in the mean age of patient groups. Differences in gender distribution were tested using Fisher's exact test. Inter-rater reliability was calculated using Cohen's kappa. With the clinical diagnosis as standard of reference, sensitivity and specificity of CT for the diagnosis of CPPD were calculated for each CT rater individually. A quantitative analysis of all imaging characteristics was performed, counting all characteristics as present, which were observed on one or both sides. Fisher's exact test was used to detect differences in frequency between CPPD and control group.

Based on the literature research the following findings were defined as '*established imaging characteristics*' and summarised into sum scores: OA of the scapho-radial and STT joints, drooping osteophytes of the MCP joints, cysts of the scaphoid and lunate bones as well as calcifications of the luno-triquetral

Table I. Grading system for image evaluation.

	OA	Drooping osteophytes	Calcifications	Cysts	Erosions	SL distance	Scaphoid subluxation
0	None	None	None	None	None	0–2 mm	Scaphoradial angle ≤70°
1	Doubtful	osteophyte ≥3 mm	calcification of cartilage only	1–2 small cysts	1–2 small erosions	3–5 mm	Scaphoradial angle ≥70°
2	Minimal		calcification of ligament only	>3 small cysts OR very large cyst (≥3 mm)	>3 small erosions OR very large erosion (≥3 mm)	5–9 mm	
3	Moderate		calcification of both cartilage and ligament			≥10 mm	
4	Severe						

OA: osteoarthritis; SL: scapho-lunate.

joint and the triangular fibrocartilage. These sum scores underwent receiver operating curve (ROC) analyses with calculations of areas under the curves (AUC) to determine the diagnostic accuracy of the findings, which are commonly described as classical hallmarks of CPPD arthropathy. Additionally, sum scores of all imaging findings with a statistically significant higher prevalence in the CPPD group were to be calculated and analysed correspondingly. The ROC analyses were carried out for each CT rater individually. A two-tailed significance level of $p<0.05$ was applied to all statistical analyses. Due to the explorative nature of this pilot study we refrained from an alpha-error correction.

Results

Patients

Forty-six patients were included in this analysis – 27 patients were assigned to the CPPD group (classified as 'probable CPPD' based on the McCarty criteria), and 19 to the control group by the expert rheumatologist. Diagnoses in the control group included rheumatoid arthritis (n=11), gout (n=4), haemochromatosis (n=1), psoriatic arthritis (n=1), ulcerative colitis associated arthritis (n=1) and osteoarthritis (n=1). Mean age of patients was significantly higher in the CPPD group (68.1 years *vs*. 60.8 years, p=0.004), gender distribution was similar in both groups (55.6% men *vs*. 52.6% men, $p=0.850$).

Radiation exposure

The majority of CT scans (35 patients), were performed using just one 3D volume containing both wrist and MCP joints. In 11 instances a second acquisition was required to capture also PIP and DIP joints, when clinically symptomatic. CT examinations resulted in dose-length-products of 24 to 59.2 mGy*cm per scan and up to 118.4 mGy*cm per patient. The effective exposure per patient therefore ranged between 0.019 and 0.095 mSv.

Table IIa. CT rater 1 and clinical diagnosis.

		Clinical diagnosis		Total
		Control	CPPD	
Rater 1	Control	18	8	26
	CPPD	1	19	20
Total		19	27	46

Table IIb. CT rater 2 and clinical diagnosis.

		Clinical diagnosis		Total
		Control	CPPD	
Rater 2	Control	16	8	24
	CPPD	3	19	22
Total		19	27	46

Inter-rater agreement and sensitivity and specificity

Agreement regarding the final diagnosis between the CT raters was almost perfect (41) with a Cohens's kappa of 0.91. Measures of diagnostic accuracy were calculated with the clinical diagnosis as the standard of reference. Sensitivity was good with 70.4% for each rater, specificity was very good with 94.7% for rater 1 and 84.2% for rater 2. The corresponding contingency tables are provided as Tables IIa-b.

Descriptive analysis

Only scoring items with an agreement between both raters were used for further analyses. The overall agreement rate per item at each location was 89.6% (range: 71.7–100%).

OA was a common finding in our study population, with the carpometacarpal joint of the thumb (CMC-I) being the most frequently affected joint (64% in the CPPD *vs*. 38% in the control group). Drooping osteophytes were an altogether rare finding, with the highest frequency in the MCP-II joints of CPPD patients (30% *vs*. 28% in the control group). A graphical representation of the distribution of these findings is provided as Fig. 2.

The distribution of calcifications can be seen in Figure 3. As can be seen there, calcifications of carpal ligaments show a significantly higher prevalence in the CPPD group. The difference in prevalence was most pronounced in the scapho-lunate (76% *vs*. 18%), the luno-triquetral (62% *vs*.16%) and the STT (56% *vs*.16%) ligaments. An example of CT presentation of ligamentous calcifications can be seen in Figure 4.

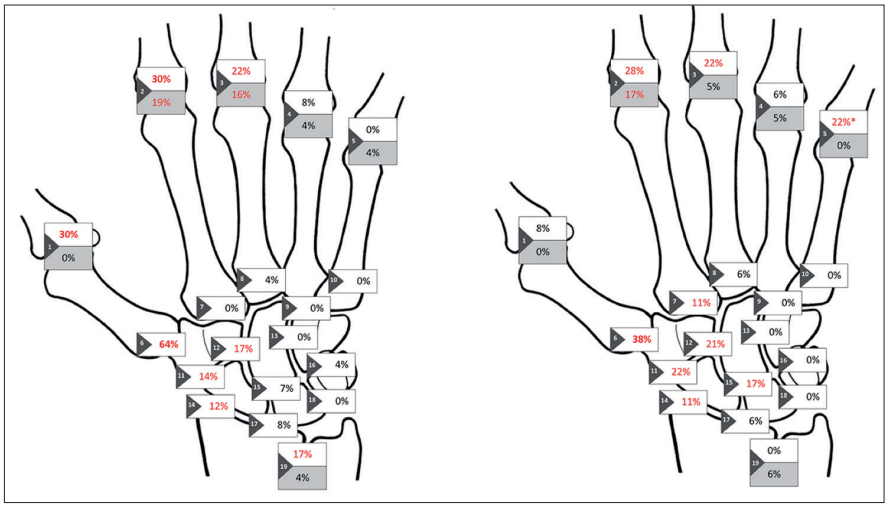

Fig. 2. Distribution of osteoarthritis and drooping osteophytes (relative) [%].
Red writing: >10% osteoarthritis / drooping osteophytes. Bold red writing: >30% osteoarthritis/drooping osteophytes. Significant difference (p<0.05) = (*). For key to locations refer to Figure 1.

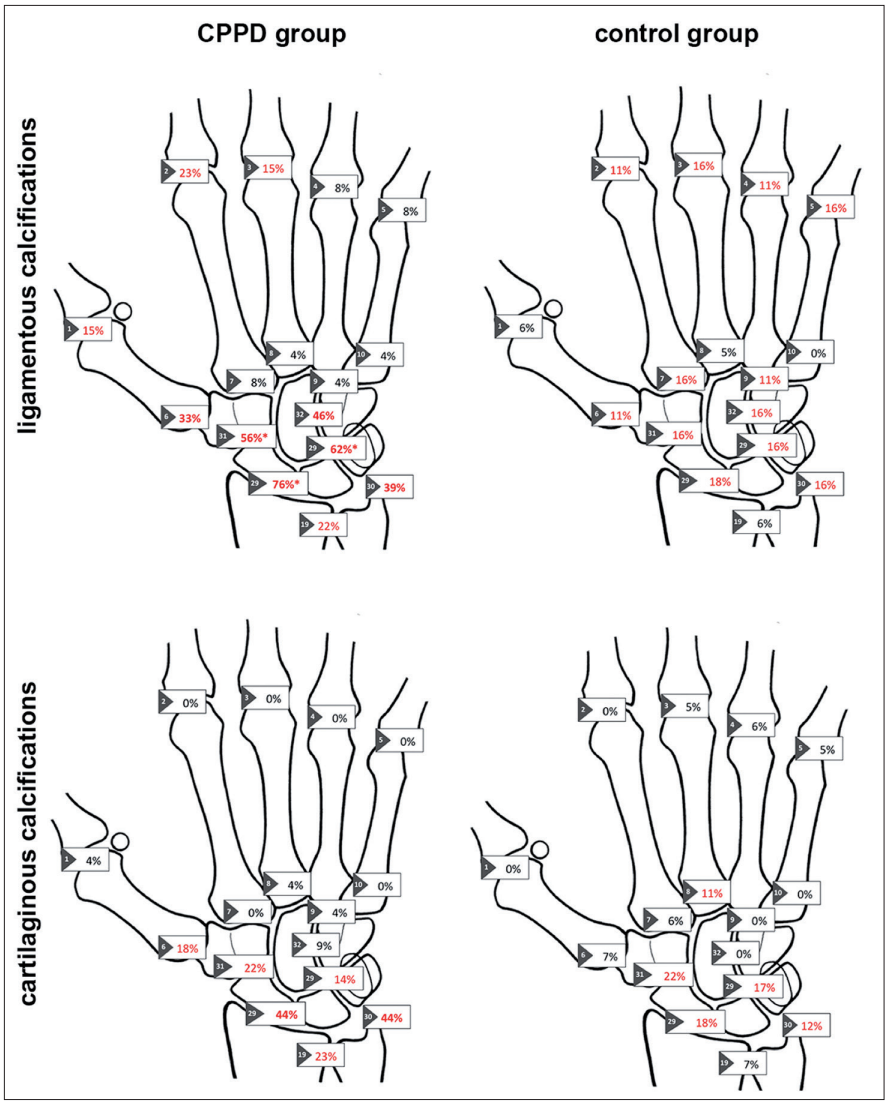

Fig. 3. Distribution of ligamentous and cartilaginous calcifications (relative) [%]. Red writing: >10% calcification. Bold red writing: >30% calcifications. Significant difference (p<0.05) = (*).
For key to locations refer to Figure 1.

Cysts and erosions were a common finding in our study population - in both groups the scaphoid, capitate and lunate were the most commonly affected bones. No significant difference in the frequency of subchondral cysts or erosions could be demonstrated.
Scapho-lunate dissociation was seen in 19% of CPPD patients and 17% of control patients. Rotary subluxation of the scaphoid was detected in 25% (CPPD) and 17% (control) of patients. There was no significant difference in the frequency of these findings.

ROC analysis
In order to explore the diagnostic value of these quantitative results further, ROC analyses on sum scores of the findings with a significantly higher frequency in the CPPD-group, namely calcifications of the scapho-lunate, luno-triquetral and STT-ligament, were carried out (maximum score=3). These were compared with the diagnostic accuracy of the sum score of the previously defined 'established characteristics' (see '*Statistical analysis*'.) (maximum score=12) – a graphical representation of both sets of findings can be seen in Fig. 5. Fig. 6 depicts the resulting receiver operating curves. The AUCs for established characteristics were 0.675 (95% CI: 0.509–0.841, p=0.049) for rater 1 and 0.619 (95% CI: 0.447–0.791, p=0.181) for rater 2. In contrast, AUCs for ligament calcifications were 0.786 (95% CI: 0.653–0.920, p=0.001) and 0.786 (95% CI: 0.652–0.921, p=0.001) for raters 1 and 2, respectively.

Discussion

This study has for the first time systematically explored the pattern of CPPD wrist arthropathy as detected using CT. We were able to identify ligamentous calcifications of the carpus as highly specific markers of the condition, and this was especially true for the scapholunate ligament, which showed calcifications in 76% of CPPD patients.
Radiographic features of OA are a widely recognised imaging characteristic of CPPD wrist arthropathy (10, 11), described as typically affecting the scapho-radial and STT joint while sparing the CMC-I joint. In our study

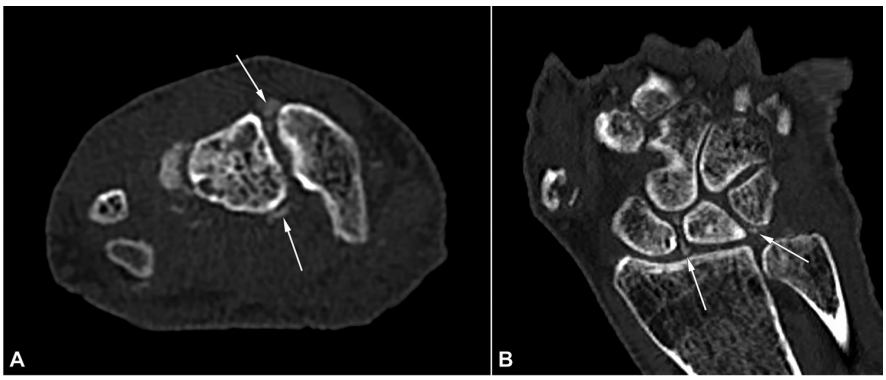

Fig. 4. Ligamentous calcifications (CT). Right carpus of 72-year-old female patient suffering from CPPD. **A**: axial reconstruction of a right wrist. **B**: curved coronal reconstruction of the same wrist. White arrows indicating calcifications of the scapholunate ligament. Calcifications of the lunotriquetral ligament can also be observed.

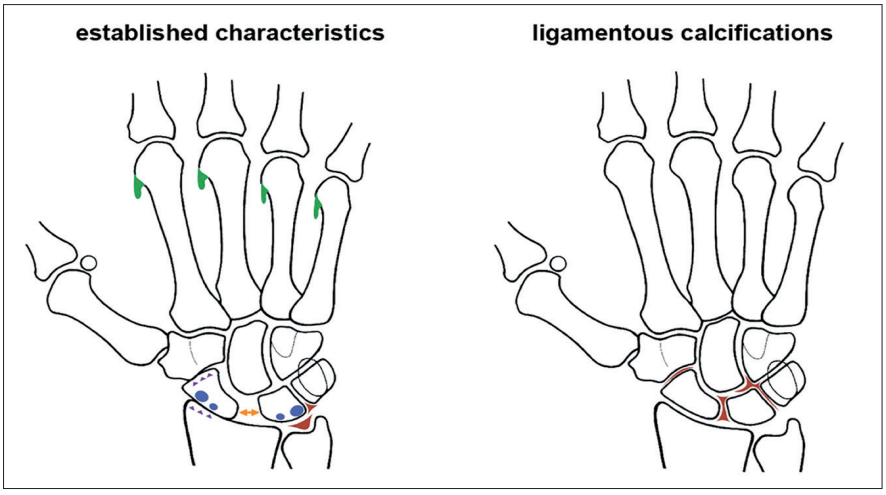

Fig. 5. Graphical representation of established characteristics and ligamentous calcifications. Established characteristics: Drooping osteophytes (green), osteoarthritis of the scapho-radial and STT joints (purple arrowheads), scapho-lunate dissociation (orange double arrow), cysts of the lunate and scaphoid (blue) and calcifications of the triangular fibrocartilage (red). Ligamentous calcifications: calcifications of the scapholunate, hamato-triquetro-luno-capital and STT joint spaces (red).

population, however, this could not be confirmed. The CMC-I was the joint most commonly affected by OA in the CPPD group, while both scapho-radial and STT manifestations were equally frequent in both groups. We therefore conclude, that the pattern of OA previously described as typical of CPPD may be less specific than was assumed. The same can be said about the drooping osteophytes (35), which were equally prevalent in both groups. Based on our data we can confirm, that CPPD is associated with cysts (13), as there was no specific pattern or significant difference in frequency however, we conclude that the development of cysts is a nonspecific sign with limited diagnostic value. The same holds true for scapho-lunate dissociation and rotary subluxation of the scaphoid, which – based on their similar frequency in both groups – also appear to be non-specific. There was no difference in the frequency of erosions between CPPD and the control group. This may in part be explained by the fact that small erosions can mimic cysts on plain radiographs (20). Another possible explanation may be the presence of a certain overlap of CPPD and rheumatoid arthritis in our study population. Recent studies have shown, that CPP crystals are detectable in the synovial fluid of up to 25.8% of patients with rheumatoid arthritis (42, 43). Previously described pathophysiological similarities to the inflammatory process of gout (44) may also explain the occurrence of bony erosions in CPPD. Further studies into the pathological mechanisms of the inflammatory processes of CPPD arthropathy are required to explain these findings.

In contrast to the imaging findings discussed above, calcifications of carpal ligaments, even more than calcifications of cartilage, were significantly more prevalent in the CPPD group. Expanding on the findings of Yang *et al*., who distinguished the luno-triquetral ligament as a predilection site of calcifications in CPPD (12), we also found calcifications in the scapho-lunate and STT ligaments in significant frequencies. The reason why the luno-triquetral ligament is the only site reliably identified as affected by calcifications up to this point might be that most prior studies have focused on solely on radiography (26), where all other carpal ligaments cannot be evaluated reliably due to superimposition. The ligament, which appears to be diagnostically most relevant based on our findings, is the scapho-lunate ligament (see also Fig. 3). Additional to their significantly more frequent occurrence in the CPPD group in our study population, the ligamentous calcifications showed a promising degree of diagnostic accuracy in the ROC analyses; markedly higher than the previously identified imaging characteristics. As the study population of this explorative analysis was rather small however, a statistically significant difference in diagnostic accuracy has not been established.

Based on these findings, we suggest, that the imaging characteristic with the greatest diagnostic value in the diagnosis of CPPD wrist arthropathy are ligamentous calcifications of the carpus. A reliable diagnostic tool for the detection of these calcifications is a low-dose CT. This is supported by a study by Misra *et al*. who demonstrated that ligamentous calcifications were a common finding in CPPD manifestations of the knee (45) and that they can be detected reliably using conventional CT. The effective radiation exposure of 0.019 to 0.095 mSv was within the range of the exposure of a standard two-plane radiograph of the hand, which has a reported exposure of 0.0002–0.1mSv (46).

Another imaging modality, which has gained increasing attention with regards to the diagnosis of CPPD is ultrasonography (47, 48). Frediani *et al*. have

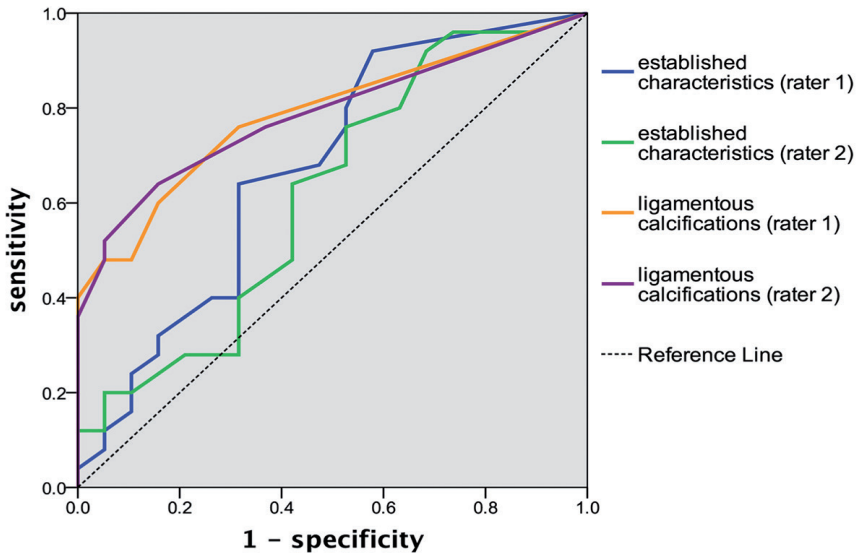

Fig. 6. ROC curve analyses. Established characteristics (blue and green lines) = OA of the STT and scapho-radial joint, cysts of the scaphoid and lunate, scapho-lunate dissociation, scaphoid subluxation, calcifications of the triangular fibrocartilage and the lunotriquetral ligament and hyaline cartilage. Ligamentous calcifications (orange and purple lines) = STT ligament, scapholunate ligament, lunotriquetral ligament – parameters were chosen based on significantly higher frequency in CPPD group (see also Fig. 3).

examined ultrasonography for the detection of articular calcifications in CPPD, and have found it to be both sensitive and specific (27). A recent study by the Outcome Measures in Rheumatology (OMERACT) CPPD Ultrasound Subtask force has attempted to define ultrasonographic criteria for manifestations at the knee and wrist (49). This and other ultrasonographic studies have largely concentrated on the characterisation of cartilage calcifications (27, 50-52) and detection of depositions in the synovial fluid (49), however, without studying frequency or pattern of ligament involvement.

As a point of discussion, it needs to be mentioned, that in this investigation we assumed that all instances of calcification were due to the deposition of calcium pyrophosphate dihydrate. As we could not draw on definitive microscopic or chemical characterisation however, calcifications may have been due to the deposition of basic calcium pyrophosphate crystals (BCPs) (53, 54). Furthermore, the patients in the CPPD group were on average 7.3 years older than their control counterparts. Even though such an unequal age distribution is to be expected in retrospective settings, given the age-dependent increase in prevalence of CPPD (55), this factor needs to be taken into account when interpreting the findings presented. The standard of reference used in this study also needs to be discussed. Due to the retrospective nature of this investigation, we were only able to draw on routine diagnostic procedures - in our study population these included only 4 arthrocenteses of the wrist. Two of these yielded no synovial fluid, one synovial analysis was inconclusive, and one detected urate crystals. Thus, we did not include any patient with "definite CPPD" in our analysis, according to McCarthy criteria (19). Whilst this failure to provide the established gold standard may weaken the accuracy of our classification into CPPD and control group, it also underlines the need for new diagnostic criteria without reliance on a diagnostic tool with challenges in daily use.

In summary, the results of this pilot study demonstrate that, by applying specific imaging criteria, low-dose CT can provide diagnostically valuable additional information in the diagnosis of CPPD with a high inter-rater reliability, and at an effective radiation exposure comparable to that of standard radiography (46). A larger prospective study comparing CT, plain radiography and ultrasonography with synovial analysis for CPP crystals as reference standard is required to establish a new and definitive set of diagnostic criteria.

Acknowledgment

The authors thank Andreas Böttner, MSc, for the statistical advice.

References

1. ABHISHEK A, DOHERTY M: Update on calcium pyrophosphate deposition. *Clin Exp Rheumatol* 2016; 34 (Suppl. 98): S32-8.
2. ZHANG W, DOHERTY M, BARDIN T *et al.*: European League Against Rheumatism recommendations for calcium pyrophosphate deposition. Part I: terminology and diagnosis. *Ann Rheum Dis* 2011; 70: 563-70.
3. SALAFFI F, DE ANGELIS R, GRASSI W; MAARCHE PAIN PREVALENCE; INVESTIGATION GROUP (MAPPING) STUDY: Prevalence of musculoskeletal conditions in an Italian population sample: results of a regional community-based study. I. The MAPPING study. *Clin Exp Rheumatol* 2005; 23: 819-28.
4. FELSON DT, ANDERSON JJ, NAIMARK A, KANNEL W, MEENAN RF: The prevalence of chondrocalcinosis in the elderly and its association with knee osteoarthritis: the Framingham Study. *J Rheumatol* 1989; 16: 1241-5.
5. MCCARTY DJ: Calcium pyrophosphate dihydrate crystal deposition disease--1975. *Arthritis Rheum* 1976; 19 (Suppl. 3): 275-85.
6. NÖTZEL A, HERMANN KG, FEIST E *et al.*: Diagnostic accuracy of dual-energy computed tomography and joint aspiration: a prospective study in patients with suspected gouty arthritis. *Clin Exp Rheumatol* 2018; 36: 1061-67.
7. SWAN A, AMER H, DIEPPE P: The value of synovial fluid assays in the diagnosis of joint disease: a literature survey. *Ann Rheum Dis* 2002; 61: 493-8.
8. ROSENTHAL AK: Update in calcium deposition diseases. *Curr Opin Rheumatol* 2007; 19:1 58-62.
9. KRIMMER H, KRAPOHL B, SAUERBIER M, HAHN P: [Post-traumatic carpal collapse (SLAC- and SNAC-wrist)--stage classification and therapeutic possibilities]. *Handchir, Mikrochir, Plast Chir* 1997; 29: 228-33.
10. FREYSCHMIDT J: Skeletterkrankungen: klinisch-radiologische Diagnose und Differentialdiagnose. *In*: HEILMANN U (Ed.) *Skeletterkrankungen: klinisch-radiologische Diagnose und Differentialdiagnose*. 1. 3. überarb. und erw. Fassung ed. Berlin, Heidelberg, New York: Springer; 2008. p. 844-51.
11. STEINBACH LS: Calcium pyrophosphate dihydrate and calcium hydroxyapatite crystal deposition diseases: imaging perspectives. *Radiol Clin North Am* 2004; 42: 185-205, vii.
12. YANG BY, SARTORIS DJ, DJUKIC S, RESNICK D, CLOPTON P: Distribution of calcification in the triangular fibrocartilage region in 181 patients with calcium pyrophosphate dihydrate crystal deposition disease. *Radiology* 1995; 196: 547-50.
13. RESNICK D, UTSINGER PD: The wrist arthropathy of "pseudogout" occurring with and without chondrocalcinosis. *Radiology* 1974; 113: 633-41.
14. STÄBLER A: [The pathophysiological etiological mechanism of destructive wrist joint arthropathy in pseudogout]. *Rofo* 1992; 156: 73-6.

15. TISCHLER BT, DIAZ LE, MURAKAMI AM *et al*.: Scapholunate advanced collapse: a pictorial review. *Insights Imaging* 2014; 5: 407-17.
16. MIKSANEK J, ROSENTHAL AK: Imaging of calcium pyrophosphate deposition disease. *Curr Rheumatol Rep* 2015; 17: 20.
17. CHANG EY, LIM WY, WOLFSON T *et al*.: Frequency of atlantoaxial calcium pyrophosphate dihydrate deposition at CT. *Radiology* 2013; 269: 519-24.
18. WARD IM, SCOTT JN, MANSFIELD LT, BATTAFARANO DF: Dual-energy computed tomography demonstrating destructive calcium pyrophosphate deposition disease of the distal radioulnar joint mimicking tophaceous gout. *J Clin Rheumatol* 2015; 21: 314-7.
19. ROSENTHAL AKRL, MCCARTY DJ: Calcium pyrophosphate crystal deposition disease, pseudogout, and articular chondrocalcinosis. *In*: KOOPMAN WJML (Ed.) *Arthritis and Allied Conditions*. 15th ed. Philadelphia: Lippincott Williams & Wilkins, 2005; p. 2373.
20. DE BUCOURT M, SCHEURIG-MÜNKLER C, FEIST E *et al*.: Cyst-like lesions in finger joints detected by conventional radiography: comparison with 320-row multidetector computed tomography. *Arthritis Rheum* 2012; 64: 1283-90.
21. NÖTZEL A, HERMANN KG, FEIST E *et al*.: Diagnostic accuracy of dual-energy computed tomography and joint aspiration: a prospective study in patients with suspected gouty arthritis. *Clin Exp Rheumatol* 2018; 36: 1061-67.
22. GOSCH D, GOSCH K, KAHN T: [Conversion coefficients for estimation of effective dose to patients from dose area product during fluoroscopy x-ray examinations]. *Rofo* 2007; 179: 1035-42.
23. SALTYBAEVA N, JAFARI ME, HUPFER M, KALENDER WA: Estimates of effective dose for CT scans of the lower extremities. *Radiology* 2014; 27: 153-9.
24. ROTHSCHILD BM: Universal nature of spondyloarthropathy as a reactive disease, reflecting differential sensitivities. *Curr Rheumatol Rev* 2013; 9: 81-9.
25. LIN YY, WANG TG, LI KJ, LEW HL: Imaging characteristics of calcium pyrophosphate dihydrate crystal deposition disease. *Am J Phys Med Rehabil* 2014; 93: 272-3.
26. MAGARELLI N, AMELIA R, MELILLO N, NASUTO M, CANTATORE F, GUGLIELMI G: Imaging of chondrocalcinosis: calcium pyrophosphate dihydrate (CPPD) crystal deposition disease -- imaging of common sites of involvement. *Clin Exp Rheumatol* 2012; 30: 118-25.
27. FREDIANI B, FILIPPOU G, FALSETTI P *et al*.: Diagnosis of calcium pyrophosphate dihydrate crystal deposition disease: ultrasonographic criteria proposed. *Ann Rheum Dis* 2005; 64: 638-40.
28. EA HK, LIOTE F: Calcium pyrophosphate dihydrate and basic calcium phosphate crystal-induced arthropathies: update on pathogenesis, clinical features, and therapy. *Curr Rheumatol Rep* 2004; 6: 221-7.
29. MADER R: Calcium pyrophosphate dihydrate deposition disease of the wrist. *Clin Rheumatol* 2004; 23: 95-6.
30. STEINBACH LS, RESNICK D: Calcium pyrophosphate dihydrate crystal deposition disease: imaging perspectives. *Curr Probl Diagn Radiol* 2000; 29: 209-29.
31. DOHERTY W, LOVALLO JL: Scapholunate advanced collapse pattern of arthritis in calcium pyrophosphate deposition disease of the wrist. *J Hand Surg Am* 1993; 18: 1095-8.
32. BERGER RA, BUCKWALTER JA: Calcium pyrophosphate dihydrate crystal deposition patterns in the triangular fibrocartilage complex. *Orthopedics* 1990; 13: 75-80.
33. ISHIKAWA K, HIGASHI I, SHIMOMURA Y, YONEMURA K: Deposition of calcium pyrophosphate dihydrate crystals in the hand. *J Hand Surg Am* 1988; 13: 943-8.
34. RESNIK CS, MILLER BW, GELBERMAN RH, RESNICK D: Hand and wrist involvement in calcium pyrophosphate dihydrate crystal deposition disease. *J Hand Surg Am* 1983; 8: 856-63.
35. ADAMSON TC, RESNIK CS, GUERRA J, VINT VC, WEISMAN MH, RESNICK D: Hand and wrist arthropathies of hemochromatosis and calcium pyrophosphate deposition disease: distinct radiographic features. *Radiology* 1983; 147: 377-81.
36. SMATHERS RL, STELLING CB, KEATS TE: The destructive wrist arthropathy of pseudogout. *Skeletal Radiol* 1982; 7: 255-8.
37. RESNICK D, NIWAYAMA G, GOERGEN TG: Comparison of radiographic abnormalities of the sacroiliac joint in degenerative disease and ankylosing spondylitis. *AJR Am J Roentgenol* 1977; 128: 189-96.
38. GENANT HK: Roentgenographic aspects of calcium pyrophosphate dihydrate crystal deposition disease (pseudogout). *Arthritis Rheum* 1976; 19 (Suppl. 3): 307-28.
39. BAHK WJ, CHANG ED, LEE AH, KANG YK, PARK JM, CHUNG YG: Huge tophaceous pseudogout associated with tenosynovial chondromatosis arising from flexor digitorum tendon sheaths of the foot: a case report. *Skeletal Radiol* 2013; 42: 1755-9.
40. KELLGREN JH, LAWRENCE JS: Radiological assessment of osteo-arthrosis. *Ann Rheum Dis* 1957; 16: 494-502.
41. VIERA AJ, GARRETT JM: Understanding interobserver agreement: the kappa statistic. *Fam Med* 2005; 37: 360-3.
42. THEILER G, QUEHENBERGER F, RAINER F, NEUBAUER M, STETTIN M, ROBIER C: The detection of calcium pyrophosphate crystals in the synovial fluid of patients with rheumatoid arthritis using the cytospin technique: prevalence and clinical correlation. *Rheumatol Int* 2014; 34: 137-9.
43. GERSTER JC, VARISCO PA, KERN J, DUDLER J, SO AK: CPPD crystal deposition disease in patients with rheumatoid arthritis. *Clin Rheumatol* 2006; 25: 468-9.
44. DALBETH N, HASKARD D: Pathophysiology of Crystal-Induced Arthritis. *In*: WORTMANN R, SCHUMACHER HJ, BECKER M, LAWRENCE M (Eds.) *Crystal-Induced Arthropathies: Gout, Pseudogout and Apatite Associated Syndromes*. New York: Taylor & Francis Group; 2006, p. 239-54.
45. MISRA D, GUERMAZI A, SIEREN JP *et al*.: CT imaging for evaluation of calcium crystal deposition in the knee: initial experience from the Multicenter Osteoarthritis (MOST) study. *Osteoarthritis Cartilage* 2015; 23: 244-8.
46. METTLER FA JR, HUDA W, YOSHIZUMI TT, MAHESH M: Effective doses in radiology and diagnostic nuclear medicine: a catalog. *Radiology* 2008; 248: 254-63.
47. FILIPPOU G, FILIPPUCCI E, TARDELLA M *et al*.: Extent and distribution of CPP deposits in patients affected by calcium pyrophosphate dihydrate deposition disease: an ultrasonographic study. *Ann Rheum Dis* 2013; 72: 1836-9.
48. FILIPPOU G, ADINOLFI A, IAGNOCCO A *et al*.: Ultrasound in the diagnosis of calcium pyrophosphate dihydrate deposition disease. A systematic literature review and a meta-analysis. *Osteoarthritis Cartilage* 2016; 24: 973-81.
49. FILIPPOU G, SCIRE CA, DAMJANOV N *et al*.: Definition and reliability assessment of elementary ultrasonographic findings in calcium pyrophosphate deposition disease: a study by the OMERACT Calcium Pyrophosphate Deposition Disease Ultrasound Subtask Force. *J Rheumatol* 2017.
50. KELLNER H, ZOLLER W, HERZER P: Ultrasound findings in chondrocalcinosis. *Z Rheumatol* 1990; 49: 147-50.
51. DI MATTEO A, FILIPPUCCI E, SALAFFI F *et al*.: Diagnostic accuracy of musculoskeletal ultrasound and conventional radiography in the assessment of the wrist triangular fibrocartilage complex in patients with definite diagnosis of calcium pyrophosphate dihydrate deposition disease. *Clin Exp Rheumatol* 2017; 35: 647-52.
52. FILIPPOU G, ADINOLFI A, CIMMINO MA *et al*.: Diagnostic accuracy of ultrasound, conventional radiography and synovial fluid analysis in the diagnosis of calcium pyrophosphate dihydrate crystal deposition disease. *Clin Exp Rheumatol* 2016; 34: 254-60.
53. KANYAKORN J, RYAN L: Clinical Manifestations of Basic Calcium Phosphate (Apatite) Deposition Disease. *In*: WORTMANN R, SCHUMACHER HJ, BECKER M, LAWRENCE M (Eds.) *Crystal-Induced Arthropathies: Gout, Pseudogout and Apatite Associated Syndromes*. New York: Taylor & Francis Group; 2006, p. 117-34.
54. FUERST M: Chondrocalcinosis. Clinical impact of intra-articular calcium phosphate crystals. *Z Rheumatol* 2014; 73: 415-9.
55. WILKINS E, DIEPPE P, MADDISON P, EVISON G: Osteoarthritis and articular chondrocalcinosis in the elderly. *Ann Rheum Dis* 1983; 42: 280-4.